

Articles

Penta- and Hexanuclear Heterometallic Carbonyl Clusters with μ_3 -O Ligands

Ludmila A. Poliakova and Sergey P. Gubin*

Institute of General and Inorganic Chemistry, Russian Academy of Sciences,
31 Leninsky Avenue, Moscow 117907, Russia

Olga A. Belyakova,* Yan V. Zubavichus, and Yuri L. Slovokhotov

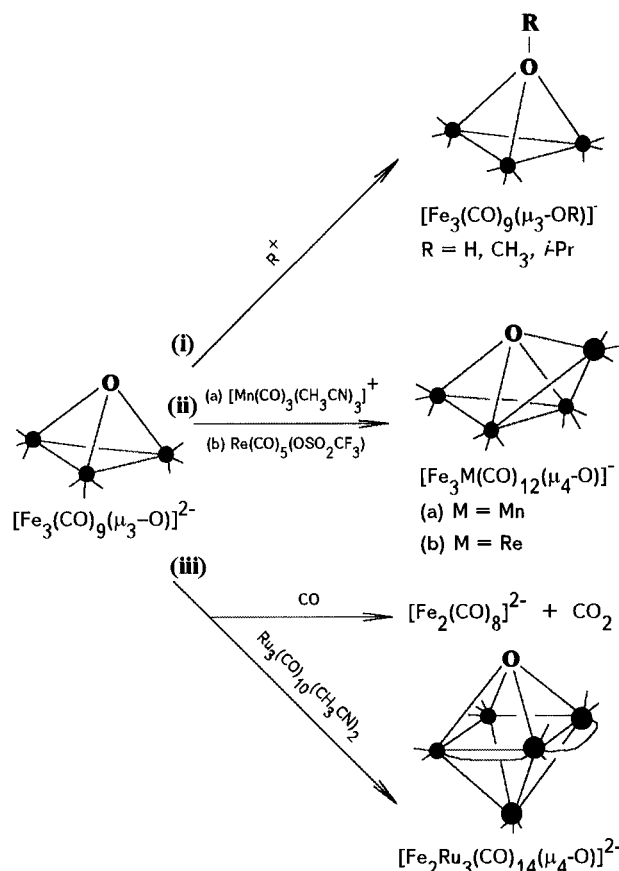
Institute of Organoelement Compounds, Russian Academy of Sciences, 28 Vavilov Street,
Moscow 117813, RussiaReceived April 22, 1997[®]

The trigonal-bipyramidal $[\text{Fe}_3\text{Au}_2(\text{CO})_{12}(\text{PPh}_3)_2(\mu_3\text{-O})]^-$ and octahedral $[\text{Fe}_3\text{Rh}_3(\text{CO})_{15}(\mu_3\text{-O})]^-$ clusters have been obtained from the reaction between a triangular $[\text{Fe}_3(\text{CO})_9(\mu_3\text{-O})]^{2-}$ cluster and metal-containing compounds $\text{Au}(\text{PPh}_3)\text{X}$ ($\text{X} = \text{Cl}, \text{NO}_3$) and $[\text{Rh}(\text{CO})_2\text{Cl}]_2$, respectively. X-ray structural studies revealed that the addition of two $\text{Au}(\text{PPh}_3)$ or three $\text{Rh}(\text{CO})_2$ groups to $[\text{Fe}_3(\text{CO})_9(\mu_3\text{-O})]^{2-}$ resulted in clusters with a virtually unchanged Fe_3 - $(\mu_3\text{-O})$ fragment.

Main-group heteroatoms in organometallic cluster compounds are generally found either in an interstitial position or on the periphery as a part of the cluster skeleton,¹ depending on the type of heteroatom. Naked C and N atoms prefer the interstitial position, while oxo, sulfide, and, in some cases, nitride ligands can be found as a peripheral component of the clusters.

Organometallic clusters containing the oxo ligand are much less numerous than organometallic carbides,² nitrides,³ and sulfides.¹ Unlike C and N, the oxo ligand has not been found in organometallic clusters in the interstitial position with high coordination numbers,⁴ though there are many examples of such oxo ligands in polyoxometalates⁵ and metallic oxo clusters.⁶ At the moment the highest known coordination number for an oxo ligand in organometallic clusters is 4, with the O atom being inside a metal butterfly core⁷ or capping the square face in the metal framework.^{8,9}

Scheme 1



In order to prepare and characterize more complicated heterometallic carbonyl clusters containing an oxo ligand, we have studied reactions of the $[\text{Fe}_3(\text{CO})_9(\mu_3\text{-O})]^{2-}$ dianion¹⁰ (1) with different metal-containing compounds. Three routes of the transformation of this

[®] Abstract published in *Advance ACS Abstracts*, September 1, 1997.

(1) Whitmire, K. H. *J. Coord. Chem.* **1988**, 17, 95.

(2) See for example: (a) Bradley, J. S. *Adv. Organomet. Chem.* **1983**, 22, 1. (b) Tachikawa, M.; Muetterties, E. L. *Prog. Inorg. Chem.* **1981**, 28, 203.

(3) Gladfelter, W. L. *Adv. Organomet. Chem.* **1985**, 24, 41.

(4) See for example: (a) Adams, S. H.; Gill, L. J.; Morris, M. J. *Organometallics* **1996**, 5, 464. (b) Shapley, J. R.; Park, J. T.; Churchill, M. R.; Ziller, J. W.; Reanan, L. R. *J. Am. Chem. Soc.* **1984**, 106, 1144. (c) Colombie, A.; Bonnet, J. J.; Fompeyrine, P.; Lovigne, G.; Sunshine, S. *Organometallics* **1986**, 5, 1154. (d) Gibson, C. P.; Huang, J. S.; Dahl, L. F. *Organometallics* **1986**, 5, 1676. (e) Goudsmit, P. R.; Johnson, B. F. G.; Lewis, J.; Raithby, P. R.; Whitmire, K. H. *J. Chem. Soc., Chem. Commun.* **1983**, 246. (f) Gibson, C. P.; Rae, A. D.; Tomchick, D. R.; Dahl, L. F. *J. Organomet. Chem.* **1988**, 340, C23. (g) Xiao, J.; Vittal, J. J.; Puddephatt, R. J.; Manojlovic-Muir, L.; Muir, K. W. *J. Am. Chem. Soc.* **1993**, 115, 7882. (h) Xiao, J.; Puddephatt, R. J.; Manojlovic-Muir, L.; Muir, K. W.; Torabi, A. A. *J. Am. Chem. Soc.* **1994**, 116, 1129. (i) Hao, L.; Xiao, J.; Vittal, J. J.; Puddephatt, R. J. *Angew. Chem., Int. Ed. Engl.* **1995**, 34, 346. (j) Xiao, J.; Hao, L.; Puddephatt, R. J.; Manojlovic-Muir, K. W. *J. Am. Chem. Soc.* **1995**, 117, 6316. (k) Uchtman, V. A.; Dahl, L. F. *J. Am. Chem. Soc.* **1969**, 91, 3763.

(5) Pope, M. T. *Heteropoly and Isopoly Oxometalates*; Springer-Verlag: Berlin, 1983.

(6) Bottomley, F.; Sutin, L. *Adv. Organomet. Chem.* **1988**, 28, 339.

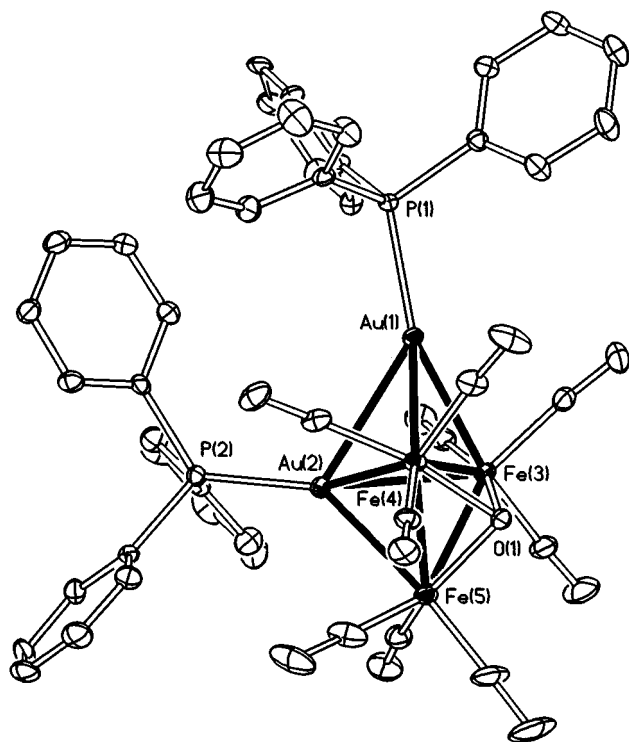


Figure 1. View of the molecular structure of the cluster $[\text{Fe}_3\text{Au}_2(\text{CO})_9(\text{PPh}_3)_2(\mu_3\text{-O})]$ (**2**) together with the atomic numbering scheme.

compound have been studied earlier^{7,8,11} (Scheme 1): (i) the addition of the organic fragment to the $\mu_3\text{-O}$ ligand, leading to $\mu_3\text{-OR}$ -containing clusters,¹⁰ (ii) the addition of the metal atom to the triangular Fe_2O face, resulting in a butterfly cluster with a $\mu_4\text{-O}$ ligand,⁷ and (iii) the formal elimination of $\text{Fe}(\text{CO})_5$ followed by transformation of the initial cluster core either to a binuclear $[\text{Fe}_2(\text{CO})_8]^{2-}$ dianion^{7b} or to a $\mu_4\text{-O}$ -containing square-pyramidal cluster.⁸

In this paper we report a fourth way of attachment of metal-containing fragments to the $\text{Fe}_3(\mu_3\text{-O})$ moiety: the simultaneous addition of different ML_n organometallic fragments to the open triangular Fe_3 face of **1**, resulting in the formation of the polynuclear clusters $[\text{Fe}_3\text{Au}_2(\text{CO})_9(\text{PPh}_3)_2(\mu_3\text{-O})]$ (**2**) and $[\text{Fe}_3\text{Rh}_3(\text{CO})_{15}(\mu_3\text{-O})]^-$ (**3**).

The reaction of $[\text{Fe}_3(\text{CO})_9(\mu_3\text{-O})]^{2-}$ and $\text{Au}(\text{PPh}_3)\text{X}$ ($\text{X} = \text{Cl}, \text{NO}_3$) in methylene chloride at 20 °C gave a solution from which the trigonal-bipyramidal cluster $[\text{Fe}_3\text{Au}_2(\text{CO})_9(\text{PPh}_3)_2(\mu_3\text{-O})]$ (**2**) was isolated in moderate yield after evaporation to dryness. The residue was chromatographed with $\text{CH}_2\text{Cl}_2/\text{hexane}$, using a 20 × 2 cm i.d. silica column. The reaction of $[\text{Fe}_3(\text{CO})_9(\mu_3\text{-O})]^{2-}$ with $[\text{Rh}(\text{CO})_2\text{Cl}]_2$ in methylene chloride or acetone at 20 °C gave $[\text{Fe}_3\text{Rh}_3(\text{CO})_{15}(\mu_3\text{-O})]^- \text{X}^+$ ($\text{X} = \text{Et}_4\text{N}$ (**3a**), PPN (**3b**)).

The structures of **2** and **3b** are shown in Figures 1

(7) See for example: (a) Schauer, C. K.; Shriver, D. F. *Angew. Chem., Int. Ed. Engl.* **1987**, *26*, 255. (b) Schauer, C. K.; Harris, S.; Sabat, M.; Voss, E. J.; Shriver, D. F. *Inorg. Chem.* **1995**, *34*, 5017.

(8) Schauer, C. K.; Voss, E. J.; Sabat, M.; Shriver, D. F. *J. Am. Chem. Soc.* **1989**, *111*, 7662.

(9) Ingam, S. L.; Lewis, J.; Raithby, P. R. *J. Chem. Soc., Chem. Commun.* **1993**, 166.

(10) Ceriotti, A.; Resconi, L.; Demartin, R.; Longoni, G.; Manassero, M.; Sansoni, M. *J. Organomet. Chem.* **1983**, *249*, C35.

(11) Bertolucci, A.; Freni, M.; Romiti, P.; Ciani, G.; Sironi, A.; Albano, V. G. *J. Organomet. Chem.* **1976**, *111*, C61.

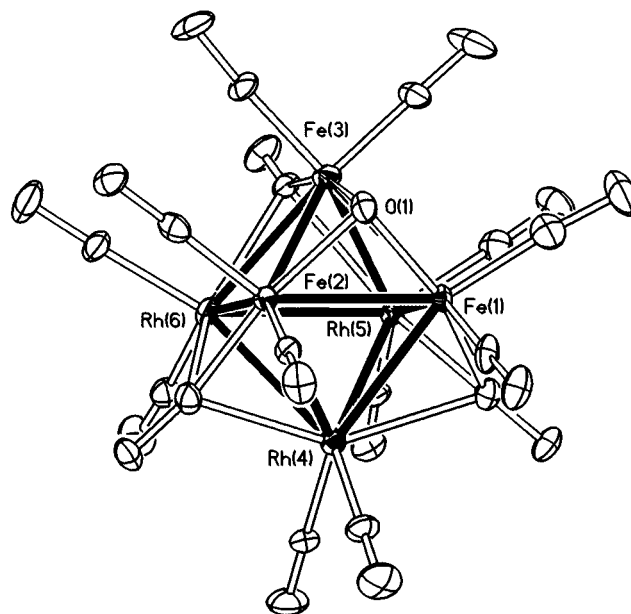


Figure 2. View of the molecular structure of the cluster anion $[\text{Fe}_3\text{Rh}_3(\text{CO})_{15}(\mu_3\text{-O})]^-$ (anion of **3b**) together with the atomic numbering scheme.

Table 1. Selected Bond Lengths (Å) and Angles (deg) for the Cluster $[\text{Fe}_3\text{Au}_2(\text{CO})_9(\text{PPh}_3)_2]$ (2**)**

Fe(3)–Fe(4)	2.700(2)	Au(2)–Fe(5)	2.688(2)
Fe(3)–Fe(5)	2.537(2)	Au(1)–Au(2)	2.9915(9)
Fe(4)–Fe(5)	2.578(2)	Fe(3)–O(1)	1.881(7)
Au(1)–Fe(3)	2.669(2)	Fe(4)–O(1)	1.875(7)
Au(1)–Fe(4)	2.714(2)	Fe(5)–O(1)	1.871(7)
Au(2)–Fe(3)	2.782(2)	Au(1)–P(1)	2.289(3)
Au(2)–Fe(4)	2.749(2)	Au(2)–P(2)	2.304(3)
Fe(3)–O(1)–Fe(4)	91.9(3)	Fe(5)–Fe(4)–Fe(3)	57.40(6)
Fe(3)–O(1)–Fe(5)	85.1(3)	Au(1)–Au(2)–Fe(3)	54.93(4)
Fe(4)–O(1)–Fe(5)	87.0(3)	Au(1)–Au(2)–Fe(4)	56.24(3)
Fe(3)–Fe(4)–Au(2)	61.38(5)	Au(1)–Fe(3)–Au(2)	66.53(4)
Fe(4)–Fe(3)–Au(2)	60.19(5)	Au(1)–Fe(3)–Fe(4)	60.73(5)
Fe(5)–Au(2)–Fe(3)	58.43(5)	Au(1)–Fe(4)–Au(2)	66.39(4)
Fe(5)–Au(2)–Fe(4)	56.60(5)	Au(1)–Fe(4)–Fe(3)	59.08(5)
Fe(5)–Fe(3)–Au(2)	60.51(5)	Fe(5)–Au(2)–Au(1)	99.66(4)
Fe(5)–Fe(3)–Fe(4)	58.89(6)	Fe(5)–Fe(3)–Au(1)	113.09(7)
Fe(5)–Fe(4)–Au(2)	60.50(5)	Fe(5)–Fe(4)–Au(1)	110.31(7)

Table 2. Selected Bond Lengths (Å) and Angles (deg) for Cluster Anion $[\text{Fe}_3\text{Rh}_3(\text{CO})_{15}(\text{O})]^-$ (3**)^a**

Fe(1)–Fe(2)	2.624(3)	Fe(2)–Rh(4)	2.691(3)
Fe(1)–Fe(3)	2.573(3)	Fe(2)–Rh(6)	2.654(3)
Fe(2)–Fe(3)	2.599(3)	Fe(3)–Rh(5)	2.670(3)
Rh(4)–Rh(5)	2.760(2)	Fe(3)–Rh(6)	2.670(3)
Rh(4)–Rh(6)	2.774(2)	Fe(1)–O(1)	1.88(1)
Rh(5)–Rh(6)	2.757(2)	Fe(2)–O(1)	1.90(1)
Fe(1)–Rh(4)	2.667(3)	Fe(3)–O(1)	1.90(1)
Fe(1)–Rh(5)	2.672(3)		
Fe(1)–O(1)–Fe(2)	87.8(5)	Fe(2)–Fe(3)–Rh(5)	92.2(1)
Fe(1)–O(1)–Fe(3)	85.9(5)	Fe(3)–Fe(1)–Rh(4)	92.33(9)
Fe(2)–O(1)–Fe(3)	86.3(5)	Fe(3)–Fe(2)–Rh(4)	91.21(9)
Fe(1)–Fe(2)–Fe(3)	59.03(9)	Fe(1)–Rh(4)–Rh(6)	87.76(7)
Fe(2)–Fe(1)–Fe(3)	59.99(9)	Fe(1)–Rh(5)–Rh(6)	88.02(7)
Rh(4)–Rh(5)–Rh(6)	60.38(5)	Fe(2)–Rh(4)–Rh(5)	88.30(7)
Rh(4)–Rh(6)–Rh(5)	59.87(5)	Fe(2)–Rh(6)–Rh(5)	89.13(7)
Fe(1)–Fe(2)–Rh(6)	91.24(9)	Fe(3)–Rh(5)–Rh(4)	88.22(7)
Fe(1)–Fe(3)–Rh(6)	92.0(1)	Fe(3)–Rh(6)–Rh(4)	87.92(8)
Fe(2)–Fe(1)–Rh(5)	91.61(9)		

^a The cation is $[\text{PPN}]^+$.

and **2**, and selected bond lengths and angles are listed in Tables 1 and 2, respectively. The cluster **2** (Figure 1) contains an Fe_3Au_2 trigonal-bipyramidal moiety with Au(1) and Fe(5) atoms in the axial positions and Au(2),

Fe(3), and Fe(4) atoms in the equatorial positions. The molecule of **2** has C_s noncrystallographic symmetry with the mirror plane passing through the atoms Au(1), Au(2), and Fe(5). The $\text{Fe}_3(\mu_3\text{-O})\text{Au}_2$ cluster core has not been observed earlier in the literature. Every Fe atom is bonded with three terminal CO groups, and the Au atoms are coordinated by PPh_3 ligands. The $\mu_3\text{-O}(1)$ atom is bonded with three Fe atoms as in the initial $[\text{Fe}_3(\text{CO})_9(\mu_3\text{-O})]^{2-}$ cluster anion. The average Fe–O distance (1.876 Å) and Fe–O–Fe bond angle (88°) in **2** are slightly different from those in **1** (1.892 Å and 82° , respectively). The Fe(3)–Fe(4) distance between two equatorial Fe atoms (2.700(2) Å) is substantially longer than the corresponding values for Fe(3)–Fe(5) (2.537(2) Å) and Fe(4)–Fe(5) (2.578(2) Å) bonds between axial and equatorial Fe atoms. The same tendency was found for Fe–Au bond lengths: 2.782(2) Å (Au(2)–Fe(3)) and 2.749(2) Å (Au(2)–Fe(4)) for two atoms in equatorial positions and 2.699(2) Å (Au(1)–Fe(3)), 2.714(2) Å (Au(1)–Fe(4)), and 2.688(2) Å (Au(2)–Fe(5)) for atoms in equatorial and axial positions.

The metal core of the cluster **2** contains 72 cluster valence electrons (CVE). The Au(1)–Au(2) distance of 2.9915(9) Å in **2** is comparable to that found for $[\text{Fe}_3(\text{CO})_9(\mu_3\text{-S})\text{Au}_2(\text{PPh}_3)_2]^{12}$ (3.020 Å) and $[\text{Ru}_3(\text{CO})_9(\mu_3\text{-S})\text{Au}_2(\text{PPh}_3)_2]^{13}$ (2.967 Å) with the same M_3Au_2 trigonal-bipyramidal moiety. These values are noticeably longer than the Au–Au bond length in metallic gold (2.884 Å) but still can be attributed to a bond.^{14–16} However, the Au–Au distance is much shorter in $[\text{Ru}_3(\text{CO})_9(\mu_3\text{-S})\text{Au}_2(\text{CH}_2\text{PPh}_2)_2]^{17}$ (2.802 Å), with a square-pyramidal $\text{M}_3\text{-CH}_2$ geometry, as well as in some other clusters.¹⁸

The structure of the cluster anion $[\text{Fe}_3\text{Rh}_3(\mu_3\text{-O})(\text{CO})_{15}]^-$ (**3**) is shown in Figure 2. The cluster anion has a C_{3v} noncrystallographic symmetry. Two parallel triangular faces, Fe(1)Fe(2)Fe(3) and Rh(4)Rh(5)Rh(6), are staggered with respect to each other, forming an $\text{Fe}_3\text{-Rh}_3$ octahedral moiety. Each Fe and Rh atom is bonded to two terminal CO ligands, and each FeRh_2 face is coordinated by a $\mu_3\text{-CO}$ ligand. The geometry of the $\text{Fe}_3(\mu_3\text{-O})$ fragment is close to that in **2**: the average values of Fe–Fe and Fe–O(1) distances and the Fe–O–Fe bond angle are 2.599 and 1.894 Å and 86° , respectively. The cluster anion $[\text{Fe}_3\text{Rh}_3(\mu_3\text{-O})(\text{CO})_{15}]^-$ has a carbido analogue $[\text{Fe}_3\text{Rh}_3(\mu_6\text{-C})(\text{CO})_{15}]^-$ (**4**) with an interstitial $\mu_6\text{-C}$ atom in Fe_3Rh_3 octahedral moiety. The average Rh–Rh distance (2.769 Å) in the $\text{Fe}_3\text{Rh}_3(\mu_6\text{-C})$ fragment

of **4** is close to that in **3** (2.764 Å), though the Fe–Fe and Fe–Rh average distances in **4** are longer (2.692 and 2.798 Å in **4**; 2.559 and 2.671 Å in **3**, respectively). Both clusters contain the equal number of cluster valence electrons (86 CVE) since the $\mu_3\text{-O}$ and $\mu_6\text{-C}$ ligands donate the same number of electrons (4e) to the cluster core.

Thus, the syntheses of **2** and **3** confirm that the oxo ligands in organometallic clusters prefer the low-coordinated peripheral position to the high-coordinated interstitial position. This tendency is probably caused by the inability of the oxo ligand to donate all its valence electrons to the cluster core.

Experimental Section

All manipulations were performed under an atmosphere of pure argon with standard techniques, and all solvents were distilled using the appropriate drying agents. Infrared spectra were recorded in CH_2Cl_2 solutions on a Specord 75IR spectrophotometer. AuPPh_3X (X = Cl, NO_3) and $[\text{Rh}(\text{CO})_2\text{Cl}]_2$ were prepared according to the published routines.^{20,21} The cluster $[\text{Fe}_3(\text{CO})_9(\mu_3\text{-O})]^{2-}$ was prepared as described previously.^{7b}

Synthesis of $[\text{Fe}_3\text{Au}_2(\text{CO})_9(\text{PPh}_3)_2(\mu_3\text{-O})]$ (2**).** 1. Solid AuPPh_3Cl (0.1131 g, 0.244 mmol) and TlBF_4 (0.122 g, 0.488 mmol) were added to a solution of $(\text{NEt}_4)_2[\text{Fe}_3(\text{CO})_9(\mu_3\text{-O})]$ (0.16 g, 0.244 mmol) in 10 mL of CH_2Cl_2 at 20 °C. The solution was stirred for 10 min and then evaporated to dryness. The residual solid was chromatographed with $\text{CH}_2\text{Cl}_2/\text{hexane}$ (1:3) using a 20×2 cm i.d. silica column. The first brown fraction was collected, and a solution was evaporated to dryness. Black crystals of **2** were obtained. Yield: 0.06 g, 18.2%. IR (CH_2Cl_2 , cm^{-1}): $\nu(\text{CO})$ stretch 2040 (m), 1990 (s), 1940 (m). Anal. Calcd: C, 44.00; H, 2.76; Fe, 12.00. Found: C, 39.88; H, 2.22; Fe, 12.41.

2. Samples of $(\text{PPN})_2[\text{Fe}_3(\text{CO})_9(\mu_3\text{-O})]$ (0.2944 g, 0.20 mmol) and $\text{AuPPh}_3\text{NO}_3$ (0.2156 g, 0.44 mmol) were dissolved in 10 mL of CH_2Cl_2 at 20 °C. The mixture was stirred for 5 min and evaporated to dryness. The residual solid was chromatographed with $\text{CH}_2\text{Cl}_2/\text{hexane}$ (1:3) using a 20×2 cm i.d. silica column. The first brown fraction was obtained, and the solution was evaporated to dryness. Black crystals of **2** were obtained. Yield: 0.1436 g, 53%. IR (CH_2Cl_2 , cm^{-1}): $\nu(\text{CO})$ stretch 2040 (m), 1990 (s), 1940 (m).

Synthesis of $(\text{NEt}_4)[\text{Fe}_3\text{Rh}_3(\text{CO})_{15}(\mu_3\text{-O})]$ (3a**).** Samples of $(\text{NEt}_4)_2[\text{Fe}_3(\text{CO})_9(\mu_3\text{-O})]$ (0.050 g, 0.0762 mmol) and $[\text{Rh}(\text{CO})_2\text{Cl}]_2$ (0.059 g, 0.1524 mmol) were dissolved in 10 mL of CH_2Cl_2 at 20 °C. The mixture was stirred for 5 min and evaporated to dryness. The residual solid was chromatographed with CH_2Cl_2 using a 20×2 cm i.d. silica column. The first brown fraction was collected, and the solution was evaporated to dryness. Black crystals of **3a** were obtained. Yield: 0.031 g, 53%. IR (CH_2Cl_2 , cm^{-1}): $\nu(\text{CO})$ stretch 2060 (w), 2025 (s), 2012 (vs), 1990 (m), 1765 (w, br). Anal. Calcd: C, 26.46; H, 1.91; N, 1.34; Fe, 16.11. Found: C, 26.88; H, 2.05; N, 1.47; Fe, 15.85.

Synthesis of $(\text{PPN})[\text{Fe}_3\text{Rh}_3(\text{CO})_{15}(\mu_3\text{-O})]$ (3b**).** Samples of $(\text{PPN})_2[\text{Fe}_3(\text{CO})_9(\mu_3\text{-O})]$ (0.16 g, 0.11 mmol) and $[\text{Rh}(\text{CO})_2\text{Cl}]_2$ (0.086 g, 0.22 mmol) were dissolved in 10 mL of acetone at 20 °C. The mixture was stirred for 10 min and evaporated to dryness, and the cluster **3b** was extracted with Et_2O (15 mL). The solution was filtered, and the filtrate was added to 15 mL of hexane. The resulting black crystals of **3b** were isolated by filtration and washed with hexane before drying under vacuum. Yield: 0.045 g, 28.7%. IR (CH_2Cl_2 , cm^{-1}): $\nu(\text{CO})$ stretch 2060 (w), 2025 (s), 2012 (vs), 1990 (m), 1765 (w,

(12) Roland, E.; Kischer, K.; Vahrenkamp, H. *Angew. Chem., Int. Ed. Engl.* **1983**, *22*, 326.

(13) Bruce, M. I.; Shawkataly, O. B.; Nicholson, B. K. *J. Organomet. Chem.* **1985**, *286*, 427.

(14) Jones, P. G. *Gold Bull.* **1986**, *19*(2), 46.

(15) Slovokhotov, Yu. L.; Struchkov, Yu. T. *J. Organomet. Chem.* **1984**, *277*, 143.

(16) See for example: (a) Ito, L. N.; Johnson, B. F.; Mueting, A. M.; Pignolet, L. H. *Inorg. Chem.* **1989**, *28*, 2026. (b) Johnson, B. F. G.; Kaner, D. A.; Lewis, J.; Rosales, M. J. *J. Organomet. Chem.* **1982**, *238*, C73. (c) Ito, L. N.; Johnson, B. F.; Mueting, A. M.; Pignolet, L. H. *Inorg. Chem.* **1989**, *28*, 2026. (d) Alvares, S.; Rossell, O.; Seco, M.; Valls, J.; Pellinghelli, M. A.; Tiripicchio, A. *Organometallics* **1991**, *10*, 2309. (e) Bruce, M. I.; Horn, E.; Humphrey, P. A.; Tiekink, E. R. T. *J. Organomet. Chem.* **1996**, *518*, 121.

(17) Brown, S. S. D.; Hudson, S.; Salter, I. D.; McPartlin, M. J. *Chem. Soc., Dalton Trans.* **1987**, 1967.

(18) See for example: (a) Rossell, O.; Seco, M.; Segales, G. *Organometallics* **1996**, *15*, 884. (b) Bunkhall, S. R.; Holden, H. D.; Johnson, B. F. G.; Lewis, J.; Pain, G. N.; Raithby, P. R.; Taylor, M. J. *J. Chem. Soc., Chem. Commun.* **1984**, 25.

(19) See for example: (a) Hriljac, J. A.; Holt, E. M.; Shriver, D. F. *Inorg. Chem.* **1987**, *26*, 2943. (b) Alami, M. K.; Dahan, F.; Mathieu, R. *J. Chem. Soc., Dalton Trans.* **1987**, 1983.

(20) Bruce, M. I.; Nicholson, B. K.; Shawkataly, O. B. *Inorg. Synth.* **1989**, *26*, 324.

(21) Cleverty, J. A.; Wilkinson, G. *Inorg. Synth.* **1966**, *8*, 211.

br). Anal. Calcd: C, 42.18; H, 2.07; N, 0.96; Fe, 11.58. Found: C, 42.30; H, 2.21; N, 1.10; Fe, 11.70.

X-ray Structure Determination. X-ray data collection was done at the center for X-ray structural studies at the Institute of Organoelement Compounds, RAS. Black rectangular crystals of **2** ($0.3 \times 0.3 \times 0.2$ mm) suitable for study by X-ray diffraction were grown by a slow diffusion of pentane into a methylene chloride solution of **2**, while black rectangular crystals of **3b** ($0.2 \times 0.1 \times 0.1$ mm) were grown from a methylene chloride/ether/hexane (1:2:1) mixture. Crystal data for **2** ($\text{C}_{45}\text{H}_{30}\text{O}_{10}\text{Au}_2\text{Fe}_3\text{P}_2$; $M_r = 1354.11$; reflection index ranges $-11 < h < 10$, $0 < k < 13$, $-46 < l < 48$; monoclinic; space group $P2_1/n$) and **3b** ($[\text{C}_{15}\text{O}_{16}\text{Fe}_3\text{Rh}_3]^-$, $[\text{C}_{36}\text{H}_{30}\text{NP}_2]^+$; $M_r = 1450.98$, including the PPN molecule; reflection index ranges $0 < k < 14$, $-14 < k < 14$, $-15 < l < 14$; triclinic; space group (from the refinement) $P\bar{1}$) are shown in Table 3. Experimental data for both crystals were collected with a Nonius CAD-4 diffractometer at room temperature: $\lambda(\text{Mo K}\alpha)$, $3\omega/5\theta$ scan, 5567 unique reflections up to $2\theta_{\text{max}} = 54^\circ$ for **2** and 6607 unique reflections up to $2\theta_{\text{max}} = 44^\circ$ for **3b**. The structures were solved by direct methods and refined by full-matrix block-diagonal least squares, using a PC version of the SHELXTL PLUS programs.²² All non-hydrogen atoms were refined in the anisotropic approximation. Hydrogen atoms were placed in calculated positions and were refined using a *riding* model. Application of absorption correction using ψ -functions for **2** (transmission from 0.066 to 0.113) and the DIFABS procedure for **2** and **3b** did not allow us to improve significantly the fit

(22) Sheldrick, G. M. SHELX-93, Program for the Refinement of Crystal Structures; University of Gottingen, Gottingen, Germany, 1993.

Table 3. Crystallographic Data for 2 and 3b

formula	$\text{C}_{45}\text{H}_{30}\text{O}_{10}\text{Au}_2\text{Fe}_3\text{P}_2$	$[\text{C}_{15}\text{O}_{16}\text{Fe}_3\text{Rh}_3]^-$ $[\text{C}_{36}\text{H}_{30}\text{NP}_2]^+$
fw	1354.11	1450.98
space group	$P2_1/n$	$P\bar{1}$
<i>a</i> , Å	8.872(2)	13.832(3)
<i>b</i> , Å	12.136(2)	13.953(3)
<i>c</i> , Å	41.568(9)	15.126(3)
α , deg	90	96.39(3)
β , deg	90.15(3)	110.56(3)
γ , deg	90	94.65(3)
<i>V</i> , Å ³	4583(1)	2694(1)
<i>Z</i>	4	2
D_{calc} , g cm ⁻³	1.962	1.789
$\mu(\text{Mo K}\alpha)$, mm ⁻¹	7.431	1.812
<i>T</i> , K	300	300
λ , Å	0.710 73	0.710 73
<i>R</i>	0.040	0.063
R_w	0.093	0.232

quality; therefore, no absorption correction of raw data was done. Final values: $R = 0.040$, $R_w = 0.093$ with 4611 non-zero reflections ($I > 4\sigma$) for **2** and $R = 0.063$, $R_w = 0.232$ with 4097 non-zero reflections ($I > 4\sigma$) for **3b**.

Acknowledgment. This work was generously supported by the Russian Foundation of Basic Researches (Grants 96-03-33245 and 96-03-32684).

Supporting Information Available: Tables of atom positional and isotropic thermal parameters, anisotropic thermal parameters, and bond distances and angles for **2** and **3b** (15 pages). Ordering information is given on any current masthead page.

OM970342M